Rotational Analysis of the $\tilde{A}^2\Pi - \tilde{X}^2\Sigma^+$ Transition of Calcium Monoacetylide, CaCCH

A. M. R. P. BOPEGEDERA, C. R. BRAZIER, AND P. F. BERNATH[1]

Department of Chemistry, University of Arizona, Tucson, Arizona 85721

The 0–0 band of the $\tilde{A}^2\Pi - \tilde{X}^2\Sigma^+$ transition of the CaCCH molecule was rotationally analyzed by dye laser excitation spectroscopy with narrow band fluorescence detection. The rotational constants extracted from the line positions enabled us to estimate the Ca–C bondlength to be 2.25 Å in the ground electronic state. This work represents the first high-resolution analysis of a metal acetylide molecule. © 1988 Academic Press, Inc.

INTRODUCTION

Our work on CaCCH is part of a series of studies of polyatomic alkaline earth metal containing free radicals (*1–14*). The "open-faced sandwich" molecules CaC_5H_5 and SrC_5H_5 were the first free radicals containing metal–carbon bonds that we discovered (*6*). More recently the $CaCH_3$, $SrCH_3$ (*11*) and CaCCH, SrCCH (*9*) molecules have been synthesized and examined under low resolution in our laboratory. A high-resolution analysis of the $\tilde{A}^2E - \tilde{X}^2A_1$ transition of the $CaCH_3$ molecule is in progress (*15*).

The analysis of the low-resolution spectra of calcium and strontium acetylides (CaCCH and SrCCH) indicated that these molecules were linear in geometry. CaCCH and SrCCH are ionic molecules, well represented by the structures $M^{+-}CCH$ (*9*). The low-resolution spectra also provided some vibrational frequencies and the spin–orbit splittings for the $\tilde{A}^2\Pi$ states.

Gruebele *et al.* have recently studied the ^-CCH ion in the gas phase using the diode laser velocity modulation spectroscopy technique (*16*). This study indicates that the C–C bondlength is longer in the ^-CCH anion compared to the CCH radical and the C_2H_2 molecule.

In our preliminary analysis of the calcium and strontium acetylide spectra, the laser-induced fluorescence was observed to be quite resonant. Many of the metal containing radicals with larger ligands have very relaxed laser-induced fluorescence, with extensive collisional redistribution of energy in the excited electronic states. The observation of resonant fluorescence allowed us to carry out a high-resolution analysis of the $\tilde{A}^2\Pi - \tilde{X}^2\Sigma^+$ transition of CaCCH, the results of which are presented here.

EXPERIMENTAL DETAILS

The method used to synthesize the CaCCH molecule has been previously described (*9*). Briefly, Ca metal was resistively heated in an alumina crucible in a Broida-type

oven (*17*) and entrained in argon carrier gas. The metal vapor was excited to the $^3P_1$ state using a dye laser and the excited metal vapor was reacted with purified welding-grade acetylene to make the CaCCH molecule. The argon pressure was 1.5 Torr with an acetylene pressure of about 10 mTorr. Unlike in the low-resolution experiment (*9*), the total pressure was maintained below 2 Torr in order to minimize collisional relaxation.

The 5-W all lines output of a cw Coherent Innova 90 argon ion laser was used to pump a broadband (1 cm^{-1}) dye laser. The wavelength of this laser was kept constant at 6573 Å to excite the $^3P_1$–$^1S_0$ atomic transition of calcium. The 7-W, 4880 Å output of a cw Coherent Innova 20 argon ion laser was used to pump a Coherent 699-29 computer-controlled single mode (1 MHz bandwidth) ring dye laser. Both dye lasers were operated with DCM dye. The output of the single mode dye laser excited the $\tilde{A}^2\Pi$–$\tilde{X}^2\Sigma^+$ electronic transition of the CaCCH molecule. An iodine cell (*18*) was used to calibrate the wave meter of the ring dye laser. The two dye laser beams were spatially overlapped and directed vertically into the Broida oven.

Initially, high-resolution laser excitation spectra of both the $\tilde{A}^2\Pi_{1/2}$–$\tilde{X}^2\Sigma^+$ and the $\tilde{A}^2\Pi_{3/2}$–$\tilde{X}^2\Sigma^+$ spin components were recorded to search for bandheads. In this experiment, the broadband dye laser was tuned to the calcium atomic line and the single mode ring dye laser was scanned over a wide region of the spectrum. The signal was detected using a photomultiplier with a 500 Å band-pass filter centered at 6500 Å. The atomic line was chopped and the modulated signal was lock-in-detected and recorded.

For CaCCH, the strong bandheads in the $\tilde{A}^2\Pi_{1/2}$–$\tilde{X}^2\Sigma^+$ spin component are Q_{12} and P_{11} while for the $\tilde{A}^2\Pi_{3/2}$–$\tilde{X}^2\Sigma^+$ spin component they are Q_{22} and P_{21} (Fig. 1). The spin–orbit splitting in the $\tilde{A}^2\Pi$ state of CaCCH is about 70 cm^{-1} so the $\tilde{A}^2\Pi$ state conforms to Hund's case (a) coupling. The notation described by Herzberg (*19*) for a $^2\Pi$–$^2\Sigma^+$ transition is used in this paper. In the excitation spectrum of the $\tilde{A}^2\Pi_{1/2}$–$\tilde{X}^2\Sigma^+$ spin component, five bandheads were observed. Of these, the one with the lowest transition energy was the strongest. A set of two bandheads appeared at 1.22 cm^{-1} higher in energy from the first bandhead, and a third set of two bandheads was observed 1.33 cm^{-1} higher than the second set of bandheads. Of these, the strongest bandhead (the one with the lowest energy) was assigned as the 0–0 band. In the excitation spectrum of the $\tilde{A}^2\Pi_{3/2}$–$\tilde{X}^2\Sigma^+$ spin component five bandheads were also observed. The separations between the bandheads were similar to those in the $\tilde{A}^2\Pi_{1/2}$–$\tilde{X}^2\Sigma^+$ spin component (approximately 1.3 cm^{-1}) except that the feature with the lowest transition energy was the weakest of the five. Initially, the transitions associated with the four strong bandheads were rotationally analyzed but the ground state combination differences did not match with those obtained from the $\tilde{A}^2\Pi_{1/2}$–$\tilde{X}^2\Sigma^+$ spin component. Finally the rotational analysis of the weakest bandhead (with the lowest energy) provided ground state combination differences which agreed with those recorded from the other spin component. Therefore this bandhead was assigned to the 0–0 bandhead of the $\tilde{A}^2\Pi_{3/2}$–$\tilde{X}^2\Sigma^+$ spin component.

Once the 0–0 component of the $\tilde{A}^2\Pi_{1/2}$–$\tilde{X}^2\Sigma^+$ transition was located, the mono-chromator (a 0.64-m monochromator with slits adjusted to provide a 0.5-Å resolution) was set on the unresolved Q_{12}, P_{11} bandhead. By scanning the single mode laser, the rotational lines (R_{12}, Q_{11}) which connect to the bandhead selected by the monochro-
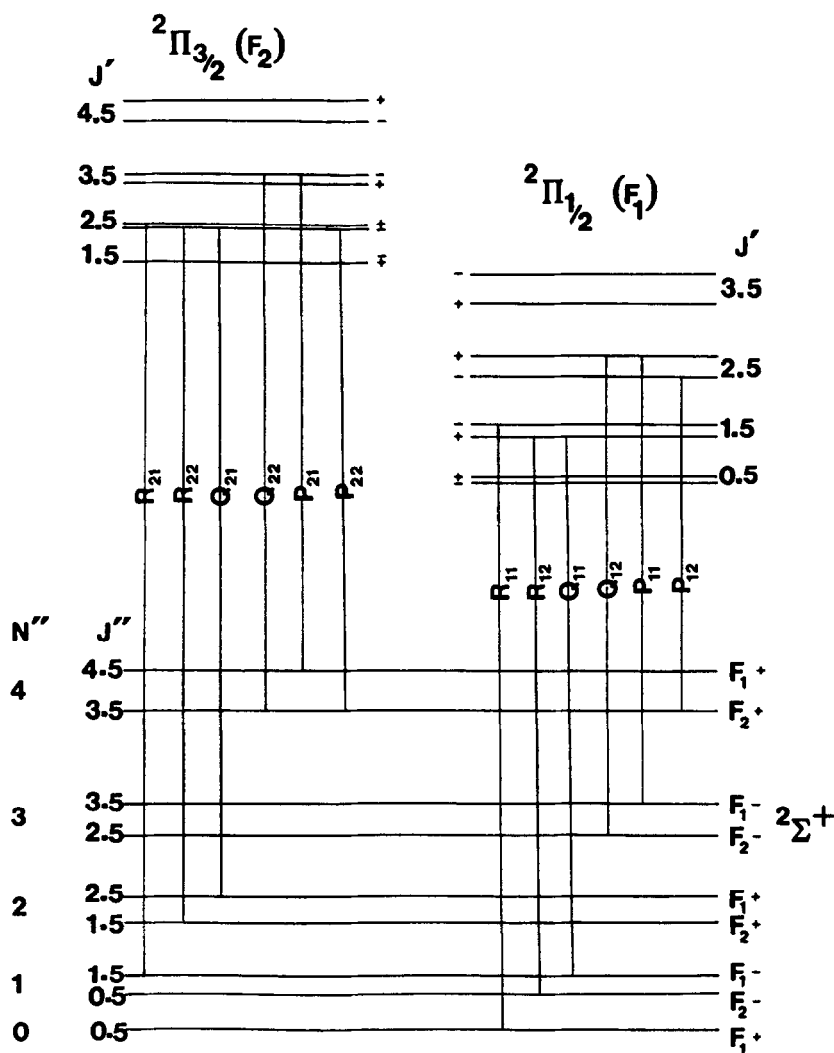
FIG. 1. Energy level diagram for a $^2\Pi$ (case a)–$^2\Sigma^+$ (case b) transition (19). Although spin–rotation doubling in the $^2\Sigma^+$ state and Λ doubling in the $^2\Pi$ state are shown in this figure, the effects of spin–rotation were not observed in the spectrum of CaCCH (see text).

mator were recorded. This method, known as the narrowband-pass detection technique, was used to record the rotational lines of a total of eight branches of the $\tilde{A}^2\Pi$–$\tilde{X}^2\Sigma^+$ transition of CaCCH. Only 8 of the 12 possible branches were observed because spin-rotation doubling of the $\tilde{X}^2\Sigma^+$ state was not resolved.

Finally, in order to obtain rotational assignments, the monochromator was set on an individual rotational line with slits adjusted to provide the highest possible resolution (about 0.2 Å). The ring laser was then scanned through the connecting branch in order to pick out the single connecting rotational line. The ground state combination

differences calculated from these connections provided definitive rotational assignments. The accuracy of the line positions is approximately ± 0.003 cm^{-1}.

RESULTS AND DISCUSSION

The energy level diagram for a $^2\Pi$ (case a)–$^2\Sigma^+$ (case b) transition is shown in Fig. 1 *(19)*. There are four branches per spin component "$-3B$", "$-B$", "$+B$", and "$+3B$". In the $\tilde{A}^2\Pi_{1/2}$–$\tilde{X}^2\Sigma^+$ spin component, the R_{11} lines are separated by $3B$ near the origin ("$+3B$ branch") while for the R_{12} and Q_{11} branches, the lines are separated by B ("$+B$ branch"). As indicated in Fig. 1, the lines of the R_{12} and Q_{11} branches are separated by the spin–rotation doubling in the ground electronic state. For the CaCCH molecule, this spin–rotation doubling was not resolved even for the highest observed rotational levels ($N'' = 63$). In the Q_{12} and P_{11} branches, the lines are separated by B ("$-B$ branch"). The lines of these two branches, which are also separated by the spin–rotation doubling in the ground state, were not resolved. The $-B$ branch forms a blue degraded bandhead at approximately $N'' = 21$ in the $\tilde{A}^2\Pi_{1/2}$–$\tilde{X}^2\Sigma^+$ transition and at $N'' = 26$ in the $\tilde{A}^2\Pi_{3/2}$–$\tilde{X}^2\Sigma^+$ transition. The lines of the P_{12} branch are separated by $3B$ ("$-3B$ branch"). The corresponding $+3B$ (R_{12}), $+B$ (R_{22}, Q_{21}), $-B$ (Q_{22}, P_{21}), and $-3B$ (P_{22}) branches of the $\tilde{A}^2\Pi_{3/2}$–$\tilde{X}^2\Sigma^+$ transition are also marked in Fig. 1.

Figure 2 is a high-resolution spectrum of the P_{12} branch ($-3B$ branch) of the $\tilde{A}^2\Pi_{1/2}$–$\tilde{X}^2\Sigma^+$ transition. These individual rotational lines have a separation of approximately $3B$ (0.3 cm^{-1}). A total of 282 lines were measured in eight branches and are reported in Table I.

The rotational line positions were fitted with a standard $\hat{N}^2$ Hamiltonian described by Brown *et al.* *(20)* for $^2\Pi$ and $^2\Sigma$ states. An explicit listing of the matrix elements used is found in a paper by Amiot *et al.* *(21)*. Initially the rotational lines of each spin component were fitted separately. For the final fit all the rotational lines were fitted
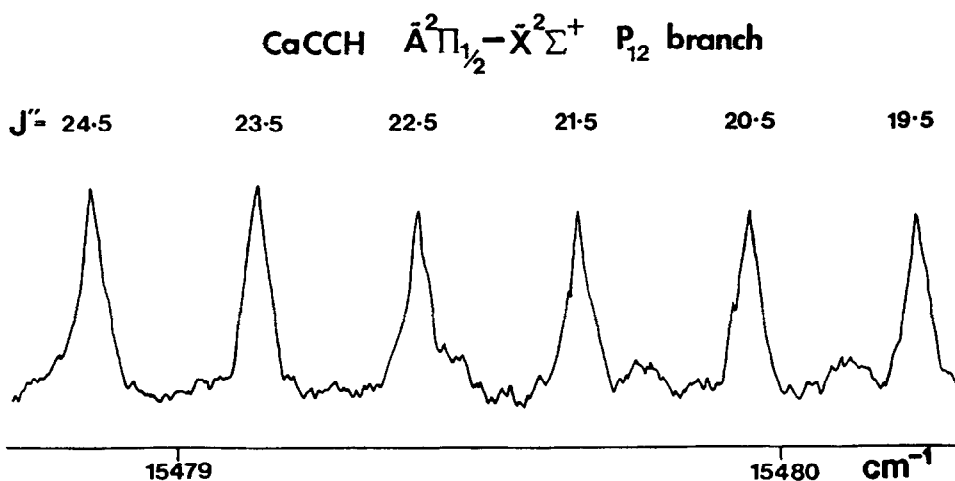

FIG. 2. The P_{12} branch ($-3B$ branch) of the $\tilde{A}^2\Pi_{1/2}$–$\tilde{X}^2\Sigma^+$ transition of CaCCH. This scan was recorded using the narrowband-pass detection technique. The monochromator was set to pass the fluorescence of the connecting $+B$ branches (Q_1 and R_{12}). The individual rotational lines are separated by approximately $3B$.

TABLE I

Observed Line Positions in the 0–0 Band of the $\tilde{A}^2\Pi-\tilde{X}^2\Sigma^+$ Transition of CaCCH (in cm^{-1})

A J	R_{22}, Q_{11}	expt-calc	P_{22}	expt-calc	R_{21}	expt-calc	Q_{22}, P_{21}	expt-calc
11.5			15552.5833	-0.0097				
12.5	15558.5499	-0.0034	15552.2981	-0.0045				
13.5	15558.7242	-0.0059	15552.0146	-0.0022				
14.5	15558.9108	-0.0007	15551.7343	-0.0012				
15.5	15559.0958	-0.0016	15551.4571	-0.0017				
16.5	15559.2868	-0.0009	15551.1836	-0.0030				
17.5	15559.4778	-0.0047	15550.8900	-0.0290	15563.4222	0.0048		
18.5	15559.6804	-0.0014	15550.6416	-0.0143	15563.8480	0.0001		
19.5	15559.8881	0.0026	15550.4003	0.0029	15564.2850	0.0022	15555.2579	0.0009
20.5	15560.0931	-0.0006	15550.1424	-0.0011	15564.7238	0.0017	15555.2396	0.0055
21.5	15560.3142	0.0079	15549.8937	-0.0004	15565.1673	0.0014	15555.2191	0.0034
22.5	15560.5166	-0.0068	15549.6513	0.0021	15565.6109	-0.0031	15555.2058	0.0041
23.5	15560.7478	0.0029	15549.4123	0.0035	15566.0659	-0.0006	15555.1973	0.0050
24.5	15560.9679	-0.0029	15549.1672	-0.0058	15566.5179	-0.0054	15555.1953	0.0080
25.5	15561.1981	-0.0029	15548.9368	-0.0049	15566.9882	0.0037	15555.1904	0.0036
26.5	15561.4339	-0.0019	15548.7121	-0.0028	15567.4502	0.0001	15555.1927	0.0020
27.5	15561.6736	-0.0013	15548.4936	0.0009	15567.9173	-0.0027	15555.1986	-0.0005
28.5	15561.9180	-0.0004	15548.2756	0.0007	15568.3933	-0.0009	15555.2089	-0.0030
29.5	15562.1626	-0.0036	15548.0621	0.0004	15568.8676	-0.0051	15555.2236	-0.0056
30.5	15562.4170	-0.0014	15547.8453	-0.0076	15569.3528	-0.0027	15555.2461	-0.0048
31.5	15562.6743	-0.0007	15547.6442	-0.0044	15569.8464	0.0039	15555.2789	0.0019
32.5	15562.9357	-0.0002	15547.4474	-0.0015	15570.3334	-0.0005	15555.3007	-0.0068
33.5	15563.2079	0.0068	15547.2505	-0.0030	15570.8362	0.0068	15555.3414	-0.0010
34.5	15563.4714	0.0008	15547.0620	-0.0007	15571.3332	0.0039	15555.3768	-0.0049
35.5	15563.7462	0.0018	15546.8720	-0.0043	15571.8313	-0.0019	15555.4245	-0.0008
36.5	15564.0205	-0.0020	15546.6874	-0.0069	15572.3454	0.0039	15555.4724	-0.0010
37.5	15564.3024	-0.0025	15546.5156	-0.0013	15572.8578	0.0039	15555.5266	0.0008
38.5	15564.5985	0.0069	15546.3411	-0.0027	15573.3762	0.0057	15555.5843	0.0018
39.5	15564.8879	0.0055	15546.1753	0.0002	15573.8956	0.0043	15555.6554	0.0119
40.5	15565.1831	0.0056	15546.0063	-0.0046	15574.4195	0.0034	15555.7060	-0.0029
41.5	15565.4787	0.0019	15545.8462	-0.0049	15574.9537	0.0086	15555.7830	0.0044
42.5	15565.7855	0.0052	15545.6849	-0.0107	15575.4870	0.0087	15555.8566	0.0040
43.5	15566.0936	0.0057	15545.5370	-0.0076	15576.0216	0.0061	15555.9371	0.0063
44.5	15566.4105	0.0107	15545.3986	0.0008	15576.5682	0.0115	15556.0099	-0.0034
45.5	15566.7258	0.0100	15545.2485	-0.0070	15577.1176	0.0156	15556.1026	0.0025
46.5	15567.0373	0.0014	15545.0896	-0.0279	15577.6644	0.0130	15556.1931	0.0020
47.5	15567.3634	0.0032	15544.9511	-0.0328	15578.2177	0.0130	15556.2819	-0.0045
48.5	15567.6906	0.0021			15578.7614	-0.0007	15556.3842	-0.0016
49.5	15568.0292	0.0083			15579.3235	0.0001	15556.4840	-0.0054
50.5					15579.8923	0.0036	15556.5953	-0.0020
51.5					15580.4562	-0.0017	15556.7064	-0.0028
52.5					15581.0277	-0.0033	15556.8208	-0.0046
53.5					15581.6067	-0.0014	15556.9369	-0.0087
54.5					15582.1865	-0.0024	15557.0675	-0.0025
55.5					15582.7730	-0.0007	15557.2557	0.0573
56.5					15583.3568	-0.0054	15557.3416	0.0106
57.5					15583.9515	-0.0031	15557.4773	0.0097
58.5					15584.5486	-0.0022		
59.5					15585.1517	0.0011		
60.5					15585.7521	-0.0022		
61.5					15586.3843	0.0227		
62.5					15586.9713	-0.0014		
63.5					15587.5778	-0.0096		
64.5					15588.2075	0.0018		

simultaneously to obtain the rotational constants reported in Table II. The Λ doubling constant p is very small and positive ($p = 0.377 \times 10^{-3}$) rather than large and negative, as would be expected from the usual $\tilde{B}^2\Sigma^+ \sim \tilde{A}^2\Pi$ interaction observed in all the other alkaline earth containing free radicals. This leads us to believe that either the $\tilde{B}^2\Sigma^+$ state is very distant from the $\tilde{A}^2\Pi$ state or, more likely, it is dissociative. This is confirmed by the fact that in our low-resolution experiments, the $\tilde{B}^2\Sigma^+-\tilde{X}^2\Sigma^+$ transition was not observed despite an extensive search in the expected region (9). The Λ doubling parameter q could not be determined from the fit and hence was fixed at zero.

TABLE I—*Continued*

B	J	P_{12}	expt-calc	R_{12}, Q_{11}	expt-calc	Q_{12}, P_{11}	expt-calc
	3.5			15486.9182	-0.0082		
	4.5			15487.0516	-0.0062	15485.8592	-0.0389
	5.5			15487.1901	-0.0024	15485.8052	0.0043
	6.5			15487.3302	-0.0005	15485.7251	0.0180
	7.5			15487.4753	0.0031	15485.6218	0.0050
	8.5	15483.2233	7.0054	15487.6170	-0.0002	15485.5350	0.0051
	9.5	15482.9047	0.0014	15487.7638	-0.0018	15485.4483	0.0019
	10.5			15487.9156	-0.0017	15485.3716	0.0053
	11.5	15482.2942	0.0097	15488.0722	-0.0003	15485.2869	-0.0028
	12.5	15481.9874	0.0071	15488.2273	-0.0037	15485.2224	0.0060
	13.5	15481.6771	-0.0024	15488.3924	-0.0005	15485.1490	0.0024
	14.5	15481.3853	0.0031	15488.5559	-0.0023	15485.0856	0.0054
	15.5	15481.0917	0.0034	15488.7210	-0.0059	15485.0156	-0.0016
	16.5	15480.7965	-0.0013	15488.8961	-0.0028	15484.9607	0.0032
	17.5	15480.5213	0.0105	15489.0712	-0.0031	15484.9007	-0.0006
	18.5	15480.2311	0.0039	15489.2492	-0.0038	15484.8455	-0.0030
	19.5	15479.9474	0.0004	15489.4298	-0.0053	15484.7939	-0.0052
	20.5	15479.6730	0.0027	15489.6149	-0.0057	15484.7423	-0.0108
	21.5	15479.3996	0.0025	15489.8067	-0.0026		
	22.5	15479.1285	0.0013	15489.9985	-0.0029		
	23.5	15478.8575	-0.0033	15490.1937	-0.0032		
	24.5	15478.5982	0.0004	15490.3938	-0.0018		
	25.5	15478.3379	-0.0004	15490.5990	0.0013		
	26.5	15478.0803	-0.0019	15490.8008	-0.0023		
	27.5	15477.8341	0.0046	15491.0092	-0.0025		
	28.5	15477.5839	0.0037	15491.2211	-0.0026		
	29.5	15477.3404	0.0061	15491.4295	-0.0094		
	30.5	15477.0904	-0.0014	15491.6580	0.0006		
	31.5	15476.8518	-0.0010	15491.8765	-0.0026		
	32.5	15476.6216	0.0045	15492.1050	0.0009		
	33.5	15476.3848	0.0000	15492.3318	-0.0006		
	34.5	15476.1613	0.0054	15492.5590	-0.0048		
	35.5	15475.9294	-0.0010	15492.7912	-0.0073		
	36.5	15475.6910	-0.0173	15493.0308	-0.0056		
	37.5	15475.4825	-0.0070	15493.2841	0.0066		
	38.5	15475.2723	-0.0018	15493.5310	0.0092		
	39.5	15475.0722	0.0101	15493.7795	0.0102		
	40.5	15474.8487	-0.0047	15494.0197	-0.0003		
	41.5	15474.6536	0.0055	15494.2465	-0.0273		
	42.5	15474.4501	0.0040	15494.5217	-0.0090		
	43.5	15474.2850	0.0376	15494.8019	0.0111		
	44.5	15474.0782	0.0262				
	45.5	15473.8630	0.0030				
	46.5	15473.6779	0.0066				
	47.5	15473.5044	0.0186				
	48.5	15473.3177	0.0140				
	49.5	15473.1359	0.0111				
	50.5	15472.9541	0.0049				

C	J	R_{11}	expt-calc
	39.5	15502.7573	-0.0060
	40.5	15503.2344	-0.0090
	41.5	15503.7247	-0.0018
	42.5	15504.2117	-0.0010
	43.5	15504.7004	-0.0015
	44.5	15505.1958	0.0017
	45.5	15505.6840	-0.0054
	46.5	15506.1858	-0.0019
	47.5	15506.6809	-0.0080
	48.5	15507.1887	-0.0044
	49.5	15507.6950	-0.0052
	50.5	15508.2064	-0.0039
	51.5	15508.7209	-0.0023
	52.5	15509.2399	0.0008
	53.5	15509.7586	0.0008
	54.5	15510.2823	0.0029
	55.5	15510.8110	0.0071
	56.5	15511.3376	0.0064
	57.5	15511.8688	0.0076
	58.5	15512.4008	0.0067

TABLE II

Rotational Constants for the 0–0 Band of the $\tilde{A}^2\Pi$–$\tilde{X}^2\Sigma^+$ Transition of the CaCCH Molecule (in cm^{-1})

Constant	$\tilde{X}^2\Sigma^+$	$\tilde{A}^2\Pi$
T_{00}	0	15 521.550 2(7)
B_0	0.115 787 88(84)[a]	0.117 778 0(80)
D_0	$0.948(23) \times 10^{-7}$	$0.107\ 2(21) \times 10^{-6}$
A_0	-	70.465 8(10)
A_{D0}	-	$0.166\ 73(70) \times 10^{-3}$
P_0	-	$0.377(34) \times 10^{-3}$

[a] Values in parentheses are one standard deviation errors from the least squares fit.

The spin–orbit coupling constant of the $\tilde{A}^2\Pi$ state was found to be 70 cm^{-1} (Table II). This value is about 4 cm^{-1} larger than the corresponding value for CaOH and is similar to the value (79 cm^{-1}) observed for CaCH$_3$ (15).

We used the rotational constants B'_0 and B''_0 obtained from our fit to calculate the Ca–C bondlength in the CaCCH molecule for the $\tilde{X}$ and $\tilde{A}$ states. In order to do this, the C–H bondlength was fixed at 1.056 Å (the value for C$_2$H$_2$ (22)) and the C–C bondlength was fixed at 1.239 Å. This C–C bondlength was calculated from the rotational constant (B''_0) of the $^-$CCH ion reported by Gruebele et al. (16) and a C–H bond distance of 1.056 Å. The ionic nature of the CaCCH molecule makes it reasonable to assume that the C–C bondlength is the same in CaCCH as in the $^-$CCH anion. The Ca–C bondlength (r_0) was calculated to be 2.248 Å for the $\tilde{X}^2\Sigma^+$ state and 2.220 Å for the $\tilde{A}^2\Pi$ state. The Ca–C and C–C bondlengths of some related molecules are

TABLE III

A Comparison of the Bondlengths of CaCCH with Some Related Molecules (in Å)

Bond		C_2H_2	$^-$CCH	CCH	CaCH$_3$	CaCCH
C-H		1.056[a]	1.056[a]	1.056[a]	1.09[c]	1.056[a]
C-C		1.204[a]	1.239[b]	1.211[d]	-	1.239[b]
Ca-C	$\tilde{X}$	-	-	-	2.353[c]	2.248
	$\tilde{A}$	-	-	-	2.341[c]	2.220

[a] Ref. (22).
[b] Ref. (16).
[c] Ref. (15) and references cited therein.
[d] Calculated from the B_0 values reported in Refs. (23, 24).

reported for comparison in Table III. The Ca–C bondlength in CaCCH is substantially shorter than the 2.35 Å observed in CaCH₃, suggesting a much stronger Ca–C bond in CaCCH.

REFERENCES

1. P. F. BERNATH AND S. KINSEY-NIELSEN, *Chem. Phys. Lett.* **105**, 663–666 (1984).

2. P. F. BERNATH AND C. R. BRAZIER, *Astrophys. J.* **288**, 373–376 (1985).

3. C. R. BRAZIER, P. F. BERNATH, S. KINSEY-NIELSEN, AND L. C. ELLINGBOE, *J. Chem. Phys.* **82**, 1043–1045 (1985).

4. C. R. BRAZIER AND P. F. BERNATH, *J. Mol. Spectrosc.* **114**, 163–173 (1985).

5. S. KINSEY-NIELSEN, C. R. BRAZIER, AND P. F. BERNATH, *J. Chem. Phys.* **84**, 698–708 (1986).

6. L. C. O'BRIEN AND P. F. BERNATH, *J. Amer. Chem. Soc.* **108**, 5017–5018 (1986).

7. C. R. BRAZIER, L. C. ELLINGBOE, S. KINSEY-NIELSEN, AND P. F. BERNATH, *J. Amer. Chem. Soc.* **108**, 2126–2132 (1986).

8. L. C. ELLINGBOE, A. M. R. P. BOPEGEDERA, C. R. BRAZIER, AND P. F. BERNATH, *Chem. Phys. Lett.* **126**, 285–289 (1986).

9. A. M. R. P. BOPEGEDERA, C. R. BRAZIER, AND P. F. BERNATH, *Chem. Phys. Lett.* **136**, 97–100 (1987).

10. A. M. R. P. BOPEGEDERA, C. R. BRAZIER, AND P. F. BERNATH, *J. Phys. Chem.* **91**, 2779–2781 (1987).

11. C. R. BRAZIER AND P. F. BERNATH, *J. Chem. Phys.* **86**, 5918–5922 (1987).

12. L. C. O'BRIEN, C. R. BRAZIER, AND P. F. BERNATH, *J. Mol. Spectrosc.*, in press.

13. C. R. BRAZIER AND P. F. BERNATH, *J. Chem. Phys.* **88**, 2112–2116 (1988).

14. L. C. O'BRIEN AND P. F. BERNATH, *J. Chem. Phys.* **88**, 2117–2120 (1988).

15. C. R. BRAZIER AND P. F. BERNATH, to be published.

16. M. GRUEBELE, M. POLAK, AND R. J. SAYKALLY, *J. Chem. Phys.* **87**, 1448–1449 (1987).

17. J. B. WEST, R. S. BRADFORD, J. D. EVERSOLE, AND C. R. JONES, *Rev. Sci. Instrum.* **46**, 164–168 (1975).

18. S. GERSTENKORN AND P. LUC, "Atlas du Spectre d'Absorption de la Molecule d'Iode," Laboratoire Amie-Cotton, CNRS 91405 Orsay, France; *Rev. Phys. Appl.* **14**, 791–794 (1979).

19. G. HERZBERG, "Spectra of Diatomic Molecules," 2nd ed., Van Nostrand–Reinhold, New York, 1950.

20. J. M. BROWN, E. A. COLBOURN, J. K. G. WATSON, AND F. D. WAYNE, *J. Mol. Spectrosc.* **74**, 294–318 (1979).

21. C. AMIOT, J. P. MAILLARD, AND J. CHAUVILLE, *J. Mol. Spectrosc.* **87**, 196–218 (1981).

22. "Handbook of Chemistry and Physics," (R. C. Weast, Ed.), 63rd ed., CRC Press, Boca Raton, FL, 1982.

23. R. J. SAYKALLY, L. VESETH, AND K. M. EVENSON, *J. Chem. Phys.* **80**, 2247–2255 (1984).

24. K. V. L. N. SASTRY, P. HELMINGER, A. CHARO, E. HERBST, AND F. C. DE LUCIA, *Astrophys. J.* **251**, L119–L120 1981.